Diatom Adhesive Mucilage Contains Distinct Supramolecular Assemblies of a Single Modular Protein

T. M. Dugdale,* R. Dagastine,† A. Chiovitti,* and R. Wetherbee*
*School of Botany, and †School of Chemical and Biomolecular Engineering, University of Melbourne, Victoria, Australia

ABSTRACT A previous study used atomic force microscopy saw-tooth retraction curves to characterize the adhesive mucilage pads of the diatom *Toxarium undulatum*. The major mucilage component consisted of adhesive nanofibers (ANFs) made up of modular proteins arranged into cohesive units, each containing a set number of modular proteins aligned in parallel. This study shows that *T. undulatum* adhesive mucilage is a biocomposite containing four additional adhesive components, including single modular proteins that are likely to be the structural units from which the ANFs are assembled. Two further distinct supramolecular assemblies were observed to coexist with ANFs (ANFs II and III), along with a continuum of single modular proteins through oligomers made up of varying numbers of modular proteins arranged in parallel. All components of the adhesive biocomposite produce a characteristic force spectrum with the same interpeak distance (35.3 ± 0.3 (mean ± SE) nm), suggesting they are derived from discrete supramolecular assemblies of the same modular protein, but they are distinguishable from one another based on the rupture force, persistence length, and interpeak force measured from their saw-tooth curves.

INTRODUCTION

Diatom cells possess complex extracellular walls composed of ornate valves sculptured from silica plus a range of mucilage coatings (1–3). The benthic marine diatom *Toxarium undulatum* Bailey (Bacillariophyceae, Ochrophyta) (4) has been found to successfully attach and grow on test panels painted with INTERSLEEK 425 (International Coatings, Akzo Nobel, Gateshead, UK), a nontoxic, foul-release coating that successfully deters most biofoulers but fails for diatoms. *T. undulatum* cells adhere by secreting adhesive mucilage from their valve poles that accumulates at the cell-substratum interface to form a distinct pad. Cells stand erect on top of the secreted pads that typically have a contact area of around 500 μm^2, which is much larger than the area of the embedded cell tip ($\sim$30 μm^2) (see Fig. 1 in Dugdale et al. (1)). As division proceeds the daughter cells usually remain attached to the parent pad, secreting additional adhesive mucilage to the expanding pad, but may detach and form a new pad. We have previously investigated the adhesive properties of these pads with atomic force microscopy (AFM) and described adhesive nanofibers (ANFs) with distinctive saw-tooth force spectra. These spectra are a reliable signature of modular proteins. In addition, protease experiments showed that the backbones of the ANFs were composed of protein (1). Experiments where cells were mechanically detached from pads showed that the ANFs were independently present in the mucilage pad and that they did not cure or otherwise alter for over 12 h after the cell was removed (1). Modular proteins consist of a long polypeptide that has multiple domains that fold into defined structures. When one end of a modular protein is anchored and the other is adsorbed to an AFM cantilever tip and pulled, the cantilever deflections result in a saw-tooth pattern as the protein mechanically unfolds. Each peak in the pattern corresponds to the rupture of the bonds holding one folded domain together, and the separation between successive peaks corresponds to the length of the unfolded domain.

Dugdale et al. (1) hypothesized that the ANFs of *T. undulatum* were made up of a set number of modular proteins aligned in parallel, forming a cohesive unit. This hypothesis was proposed because the force required to unfold the domains (790 pN) and the persistence length of the fiber (0.03 nm) derived from the worm-like chain (WLC) model of polymer elasticity (5) were not consistent with those previously recorded from the mechanical unfolding of single modular proteins with AFM ($\sim$100–300 pN and $\sim$0.2–0.4 nm, respectively). The high rupture force and low persistence length are instead consistent with how these parameters are expected to behave when multiple molecules in parallel are stretched. In addition, the ANFs could be repeatedly stretched and relaxed, resulting in saw-tooth spectra that superimposed for hundreds of stretch-relax cycles. This repeatability provided evidence that the adhesive being stretched was a single, cohesive unit rather than a variable number of strands or molecules associating in a nonspecific way. In this study, we further investigated the adhesive mucilage of *T. undulatum* and provide further compelling evidence that the ANFs are made up of multiple modular proteins aligned in parallel. We also provide strong evidence that the adhesive mucilage of the pad is a complex biocomposite containing a range of distinct stable assemblies comprising the same modular protein.

Submitted December 4, 2005, and accepted for publication January 6, 2006.

Address reprint requests to Dr. R. Wetherbee, School of Botany, University of Melbourne, Parkville, VIC 3010, Australia. E-mail: richardw@unimelb.edu.au.

0006-3495/06/04/2987/07 $2.00

doi: 10.1529/biophysj.105.079129

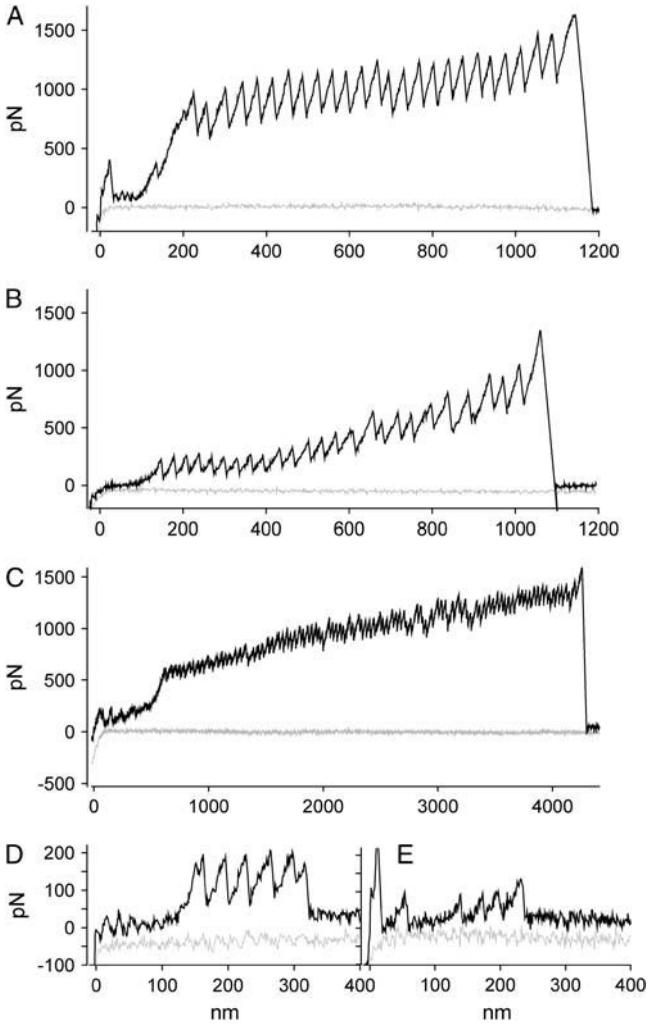

FIGURE 1 Force curves representing the unfolding of typical (*a*) ANF I, (*b*) ANF II, (*c*) ANF III, (*d*) oligomers, and (*e*) monomers. Black lines, retraction curves; gray lines, advancing curves. Note the different scales.

METHODS

Diatom culture

T. undulatum cells were isolated into clonal culture from panels coated with INTERSLEEK 425 in Port Phillip Bay, Melbourne that were provided by the Defense Science and Technology Organization (DSTO; Melbourne, VIC, Australia). *T. undulatum* cells were grown under static conditions in 250 ml conical flasks containing 100 ml K medium-containing silicates (6) inside a growth cabinet at 16°C with a 16:8 h light:dark cycle.

Atomic force microscopy

T. undulatum cells were prepared for the AFM by inoculating them into tissue culture petri dishes containing the same medium as above and returned to the culture conditions for 48 h. The petri dishes were then positioned on the stage of an Asylum MFP-3D AFM (Asylum research, Santa Barbara, CA) equipped with oxide-sharpened (typical radius of curvature <20 nm) 'V'-shaped Si_3N_4 cantilevers (Park Scientific Instruments, Sunnyvale, CA) with measured spring constants ((7); second longest = 0.041 ± 0.002 (mean ± SE) N/m; third longest = 0.103 ± 0.028 (mean ± SE) N/m), and raw curves were converted to force versus separation with the Asylum software. The cantilever was guided over a diatom mucilage pad with an optical microscope. In force mode, the cantilever tip was lowered toward the mucilage pad while recording deflection versus distance curves. A similar method has been used before and was termed 'fly-fishing' (1,8). The position of the individual pads probed with the AFM were then marked within the petri dish, which was then returned to the growth cabinet and observed over another 24 h to ensure the cells attached to the mucilage pads continued to divide and act normally. This ensured that cells remained alive after the AFM measurements and also allowed us to probe the same pads over time.

After a curve was recorded on the pad the tip was retracted, while continuing to scan, to ensure the mucilage was detached and then moved to a new *x-y* position where the procedure was repeated. Ramp was set from 1–5 μm with a scan rate of 0.5 Hz.

Force versus separation curve analysis

The WLC fitting function in the Asylum operating software (IGOR pro 5.03; MFP3D Xop build 23 up1) was used to fit each of the peaks of the saw-tooth force versus separation curves (treated as representing an unfolded domain of a modular protein). In addition, the average rupture force, interpeak force, distance between peaks, and extension ratio were recorded and the differences between averages determined by one-way ANOVAs (SYSTAT version 7.0).

The persistence length, derived with the WLC model, divides in proportion to the number of parallel chains being stretched (5). The estimated persistence length (q_o) of the single adhesive modular protein molecule was therefore obtained from the distribution of the apparent persistence lengths (q) derived from WLC fits to many saw-tooth curves. The persistence length was identified as the length corresponding to the histogram peak of the longest apparent persistence length.

The number of molecules in the adhesive fibers can be calculated from their apparent persistence length (q) derived from the force-extension curve as

$$n = q_o/q.$$

This method is adapted from Kellermayer et al. (9,10). Implicit in this method are the assumptions that all of the fibers or molecules being stretched are composed of identical polymers and that the tethers only differ in the number of modular proteins that are aligned into the fiber.

RESULTS

Analysis of saw-tooth curves from the adhesive components

Saw-tooth curves representative of unfolding ANFs (now ANFs I) made up of modular proteins have previously been reported within the adhesive mucilage of *T. undulatum* (1). In this study, four new adhesive components are described. All produce saw-tooth curves when unfolded with an AFM that has unique characteristics that allow them to be distinguished from one another. These new components were categorized and named ANF II, ANF III, monomers, and oligomers (Fig. 1, *B–E*, respectively). These curves could be distinguished by comparing the average rupture force of the domains, the persistence length of the unfolded domains, and the increase in force between successive troughs and peaks (Figs. 2 and 3). The interpeak distance was not significantly different between all curve variants ($p = 0.624$, ANOVA; 35.3 ± 0.3 (mean + SE) nm). An additional, irregular type of curve (not illustrated) was often recorded from the adhesive

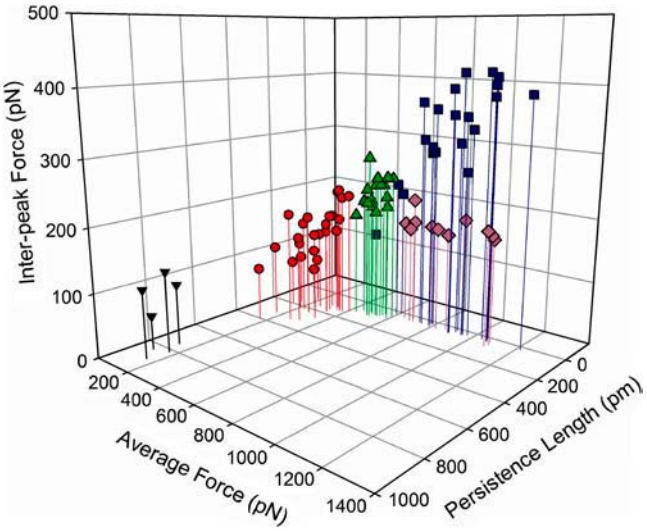

FIGURE 2 Plot of the average rupture force of the domains versus the persistence length versus the interpeak force for each of the five adhesive components (*blue squares*, ANF I; *green triangles*, ANF II; *lavender diamonds*, ANF III; *red circles*, oligomers; *black inverted triangles*, monomers).

pad that had irregular rupture peaks. These curves are thought to derive from nonspecific polymers associated with the pad mucilage, similar to the adhesive polymers recorded from other live diatoms (11–16), seaweed spores (17), bacteria (18), yeast (19,20), and fungi (21), and they were not analyzed further.

Successful determination of the persistence length based on a histogram analysis presumes that all of the stretched fibers are composed of the same polymer with the same

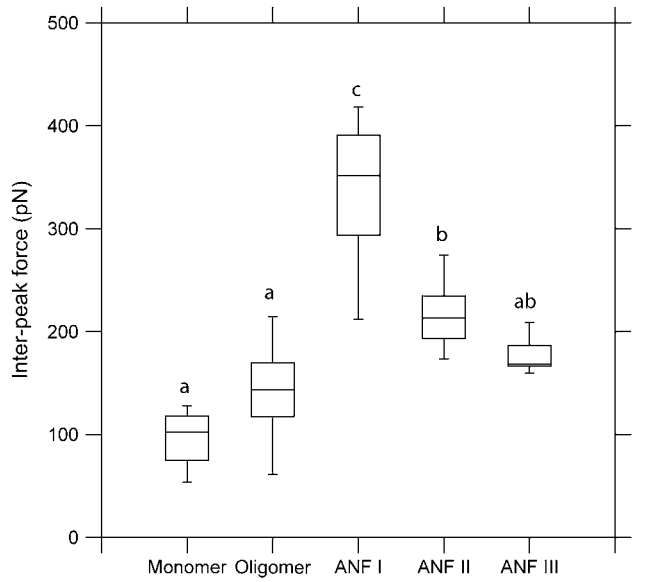

FIGURE 3 Average interpeak force between successive troughs and peaks in each of the curve types (adhesive components). Analysis was by one-way ANOVA followed by Tukey's post hoc test. Identical letters indicate no significant difference ($p > 0.05$).

persistence length and that the only difference is the number of molecules making up the fiber. We are confident that all of the saw-tooth curves shown here represent adhesive components composed of variable numbers of the same modular protein because the interpeak distance (which represents the length of polypeptide chain released when the bonds that hold the folded domain together rupture) is the same for all curves (mean, 35.3 nm). Assuming an amino acid length of 0.36 nm (22), this corresponds to ~97 amino acids present within the 35-nm-long domain. It seems unlikely that, if each of the curve variants derives from a different modular protein, the number of amino acids in the domains would be the same. Therefore, based on the histogram analysis, we assign 830 pm as the persistence length of the single modular protein (Figs. 2 and 4, Table 1). The number of modular proteins (q_o/q) in the remaining recorded curves varies from 2 to 63, with average values of each adhesive component shown in Table 1.

The persistence length data suggest that the single adhesive modular protein assembles into a range of higher order structures with variable numbers of molecules aligned in parallel. The average force is proportional to the number of molecules in a fiber/oligomer, and this relationship can be described by the equation shown in Fig. 5.

Characterization of the adhesive components

ANF I

ANF I curves (Fig. 1 *A*) have been hypothesized to represent the unfolding of a set number of modular proteins aligned in parallel and functioning as a cohesive unit (1). The persistence length analysis carried out here suggests that these ANFs are composed of ~29 modular protein molecules (Table 1). The ANFs I were present in all of the mucilage pads probed with the AFM and were the most common variant (~60% of all saw-tooth curves recorded, Table 1), indicating that these curves represent a stable supramolecular assembly.

Monomers

The authors propose that the monomer curves (Fig. 1 *E*) represent the unfolding of single modular proteins. These curves are most likely to represent single modular proteins that assemble to form the fibers that show all of the other curve variants. These curves occur extremely rarely (only four cases) in two separate mucilage pads, indicating either the monomers are not always present in the mucilage pad or they are not as adhesive as the ANFs, either because of a lack of adhesive motifs or simply because they are smaller and less likely to come into contact with the tip.

Oligomers

Persistence length analysis suggests that the adhesive component represented by oligomer curves (Fig. 1 *D*) are

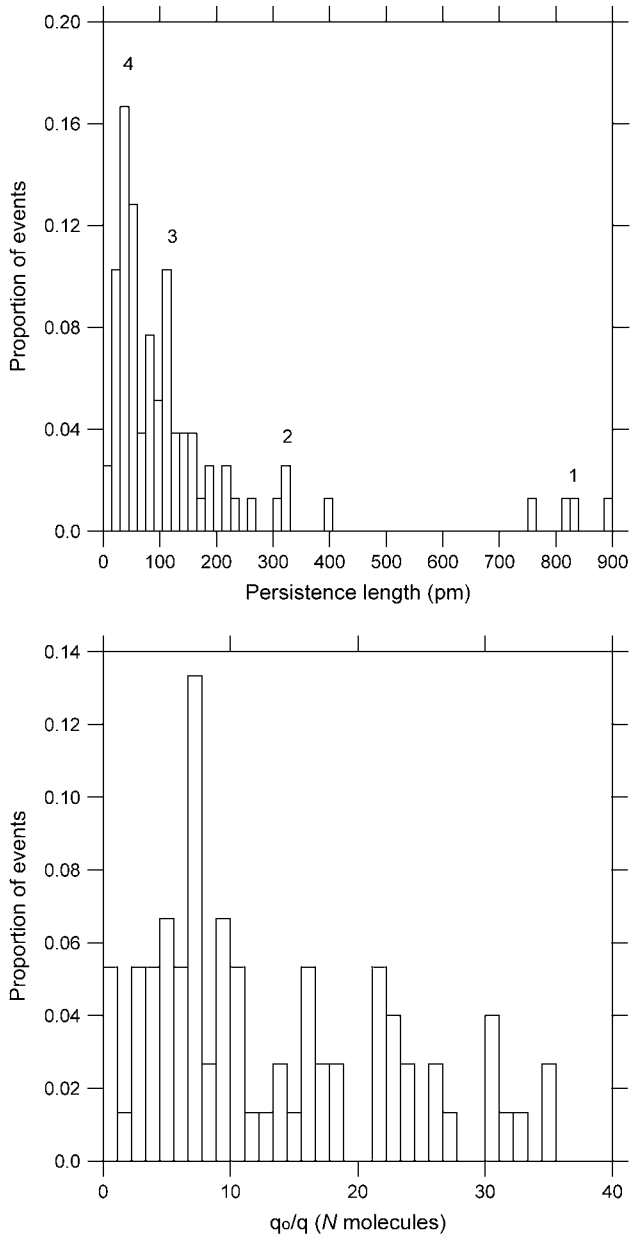

FIGURE 4 Histograms of persistence length (*top*), showing peaks at ~830 (*1*), 320 (*2*), 120 (*3*), and 40 (*4*) pm, and q_o/q (*N* of molecules per fiber/oligomer) (*bottom*). Note that the numbers in the top histogram do not represent the number of molecules; they represent the apparently stable or preferential arrangement of the monomers into supramolecular assemblies. Note that the histograms are of the curves presented in Table 1.

composed of an average of 5 (range, 2–8) single molecules. Oligomers account for ~22% of all saw-tooth curves recorded (Table 1). These curves overlay with the low force section of the ANF II curves and average 10 peaks. ANFs II also average 10 peaks in the low force region; however, the variability of the force in the oligomers is greater than the variability of the force in the low force region of ANFs II.

ANF II

The adhesive component ANF II is represented by curves that are intermediate between oligomers and ANFs I in average force, persistence length, interpeak force, and number of component molecules (Figs. 1–3, Table 1). In addition, the minimum forces of these curves are the same as the oligomer forces and the maximum forces are the same as the ANF I forces. ANF II curves occur very infrequently (~8% of all saw-tooth curves recorded; Table 1). These curves have extremely well-defined characteristics. For example, the average number of teeth and distance to the first and last teeth are all tightly clustered around their means: 24 ± 1 nm, 161 ± 16 nm, 1023 ± 33 nm (mean ± SE), respectively, representing the lowest variability of all of the adhesive components for the distance to the last peak and the number of peaks present (±3% and 2%, respectively), whereas the distance to the first peak is the second-least variable (±10%) (Table 1). In addition there are typically 10 low force peaks in the ANF II curves before the force begins to increase steeply.

The data indicate that ANFs II represent adhesive components made of ~10 (Table 1) modular proteins aligned in parallel and that they form a cohesive unit in much the same way as ANFs I do. In contrast to ANFs I, ANFs II are composed of modular proteins that do not all occur along the entire length of the fiber. The polymers that do not are either shorter or are not cross-linked with the body of the fiber and therefore don't contribute to the early, low force peaks of the curves. The final rupture force in the ANF I and ANF II curves probably results from the adhesive of the fiber detaching from the cantilever tip. This force is the same for both the ANF I and ANF II curves, indicating that they both have the same adhesive strength. The other high force peaks of the ANF II curves (the last three) have significantly lower force (ANOVA; $p < 0.004$) than the corresponding peaks of the ANF I curves (last three peaks of the ANF I curves with ≥20 peaks).

ANF III

The adhesive component ANF III is represented by curves (Fig. 1 *C*) that have the same rupture force and persistence length as ANFs but have significantly lower interpeak forces (ANOVA, $p < 0.001$) and composite number of molecules (Figs. 2 and 3, Table 1). In addition, ANFs III can be >5 μm long when unfolded, whereas the maximum extension of ANFs I is 1.2 μm. The saw-tooth pattern is not as precise as in the ANFs I (Fig. 1). It is clear that the ANFs III are different from the ANFs I and arise from a different assembly of molecules because combinations of both ANFs I and II have been recorded in a single retraction curve (Fig. 6). The ANFs III occur in only 40% of the mucilage pads. Despite this, they account for ~18% of all saw-tooth curves recorded (Table 1).

TABLE 1 Key values (±SE) recorded for each adhesive component

	Monomers	Oligomers	ANFs I	ANFs II	ANFs III
Average peak force (pN)	135 ± 16	270 ± 16	872 ± 42	516 ± 12	850 ± 168
Δ Force, trough to next peak (pN)	96 ± 16 a	143 ± 44 a	331 ± 17 c	215 ± 7 b	184 ± 36 ab
Average final peak force (pN)	148 ± 14	390 ± 41	1109 ± 86	1180 ± 63	1081 ± 426
Average first peak force (pN)	126 ± 15 (12)	200 ± 8 (4)	614 ± 28 (5)	244 ± 10 (4)	634 ± 16 (3)
Distance to first peak (nm)	287 ± 82 (29) a	284 ± 47 (16) ac	188 ± 24 (13) a	160 ± 16 (10) ad	656 ± 58 (9) b
Distance to last peak (nm)	365 ± 86 (23)	603 ± 47 (8)	691 ± 70 (10)	1023 ± 33 (3)	2253 ± 467 (21)
Distance between teeth (nm)	34.1 ± 3.0	34.8 ± 0.6	35.0 ± 0.5	35.8 ± 0.5	36.5 ± 0.8
Persistence length, q (pm)	830 ± 30	190 ± 20	30 ± 3	90 ± 5	40 ± 5
Extension ratio	0.91 ± 0.01 a	0.85 ± 0.01 ac	0.77 ± 0.02 b	0.86 ± 0.01 ac	0.81 ± 0.01 bc
Average q_o/q	1.0 ± 0.04	5.0 ± 0.4	29.4 ± 3.2	10.1 ± 0.6	20.8 ± 2.0
Average n peaks	3.3 ± 0.5 (15)	10.4 ± 1.0 (10)	15.3 ± 1.8 (12)	24.0 ± 0.5 (2)	43.3 ± 12.4 (29)
n curves analyzed	4	24	20	18	12
*% occurrence of saw-tooth curves	0.9 ± 0.7	22.4 ± 9.8	62.3 ± 27.9	7.7 ± 4.5	18.1 ± 13.4

Figures in parentheses represent the mean ± SE expressed as a percentage of the mean. Note, n represents all of the variant curves recorded on 10 mucilage pads except for ANFs II and ANFs I, where a subset of curves was analyzed. Not all monomers and oligomers were analyzed because some had nonspecific adhesion that partially obscured the curve and a subsample of the ANFs I and III were analyzed.
*As calculated from 536 saw-tooth curves recorded from 10 *T. undulatum* mucilage pads.

DISCUSSION

This work further characterizes the adhesive mucilage pads of the fouling diatom *T. undulatum* utilizing AFM. Cells of this species readily attach to marine surfaces, including manmade structures, by an adhesive biocomposite that includes at least five components, each defined by saw-tooth curves with the fingerprint of modular proteins. Curves representing single modular proteins plus four distinct supramolecular assemblies of the same modular protein were obtained, oligomers plus three types of ANFs (I, II, and III). ANFs I previously described (1) appear to be the main adhesive component of the pad mucilage, whereas the single molecules are the least abundant.

The persistence length of the monomers is 830 pm, which is in the range expected for the stretching of a single polypeptide chain with AFM (23,24). Likewise, the average rupture force of the monomer domains is 135 pN, which is also in the range previously recorded for the unfolding of single modular proteins (25–27). We are therefore confident that the monomer curves represent the unfolding of single modular proteins and that we can then use the persistence length to determine how many parallel molecules are present in the higher-order adhesive components.

During this study only four force curves representing single modular proteins were observed out of a total of ~5500 curves recorded while fly-fishing close enough to the pad surface to record ANFs or in direct contact with it. We would not expect many monomers to be present in the diatom mucilage pad, as they appear to readily self-assemble into larger fibers. The function of the pad is to provide cell-substratum attachment to hold the cell in place in its natural environment, i.e., attached to rocks and macroalgae in the ocean. It is therefore likely that this attachment mechanism has evolved to be as strong as possible so the adhesive will usually be present in the strong, flexible supramolecular assemblies, such as ANFs I, II, and III, that have the highest forces sustained over the longest distances (1–5 μm).

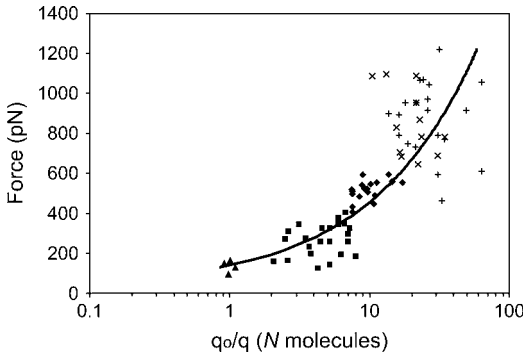

FIGURE 5 Number of molecules per oligomer/fiber (q_o/q) versus the average peak force. +, ANF I; ♦, ANF II; ×, ANF III; ■, oligomers; ▲, monomers. Curve, power trendline ($y = 127x^{0.572}$; $R^2 = 0.736$). Note log scale.

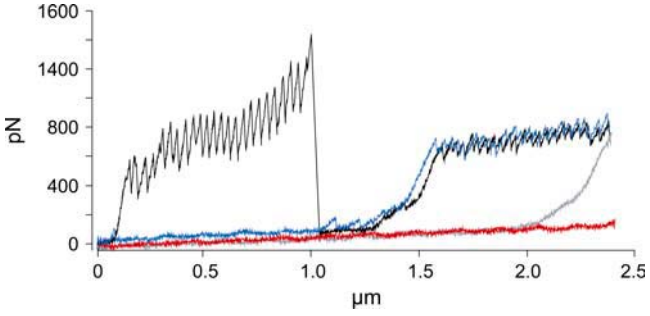

FIGURE 6 An ANF I and III (as in Fig. 1) recorded in a single retraction curve from a *T. undulatum* mucilage pad. The first extension (*red*) and retraction (*blue*) cycle represents fly-fishing where an ANF III attaches to the tip and is unfolded, then the second extension (*gray*) and retraction (*black*) cycle is repeated and an ANF I attaches to the tip and unfolds as well as the ANF III.

It is likely that the oligomer data represent the unfolding of supramolecular assemblies consisting of a continuum of composite modular proteins from monomers up to polymers, as suggested by Fig. 5. This seems most likely to occur when monomers join together in parallel to form oligomers. However, when greater numbers of molecules assemble this continuum breaks down, or at least becomes punctuated by certain supramolecular assemblies that are stable and form preferentially, giving rise to the distinct ANFs. Evidence strongly suggests that the three ANF types actually represent discrete assemblies in their own right. In this situation, where there are approximately eight or more parallel molecules present, the apparent continuum in the number of molecules between the ANFs observed in Fig. 5 is probably the result of experimental errors associated with each step of the methodology employed. For example, inherent error associated with calculating persistence lengths with WLC fits, cantilever calibration error ($\pm 10\%$), presence of partially unfolded molecules, fibers containing molecules of unequal length, parallel molecules interacting with each other, and variation of the actual persistence length along the molecule's length (9). Although each of these sources of error is likely to be small, they are likely to interact to produce scatter around a mean, especially considering that these data were recorded on native mucilage being secreted from a living cell.

The curves arising from oligomers overlay with the low force section of the ANF II curves, and it is possible that a portion of them represents the partial unfolding of an ANF II before it detaches from the tip. However, there is greater variability in the mean rupture forces of the oligomers than the ANFs II, suggesting that the former adhesive components are indeed made up of a variable number of monomers and are independent from ANFs II.

We have shown that ANFs II have very precise characteristics that are structurally distinct from the ANFs I described (1), although both nanofibers possess the same adhesive strength. The ANFs II appear to provide cells with a modular adhesive component that unfolds at lower force than that provided by ANFs I (i.e., one that is more easily extensible). The infrequent recording of the ANFs II compared to the ANFs I does not necessarily mean that they make up a small portion of the adhesive mucilage. We have shown that the ANFs I have adhesive sites along their entire length (1), whereas the reproducibility of the ANFs II data suggest that they always unfold in the same way and apparently only have a single adhesive site along the fiber's length (most likely located at the tip). Therefore, we would expect the ANFs II to come into contact with the cantilever much less frequently than ANFs I. In addition, Marszalek et al. (28) have found that the relative abundance of curve fingerprints cannot be used to estimate the relative abundance of the target molecules. They successfully used AFM fingerprints to identify individual polysaccharides from a mixture of polysaccharide species, but the relative abundance of the fingerprint curve types recorded did not match the known relative abundance of each polysaccharide species in the sample.

ANFs III have the same unfolding force and persistence length as ANFs I but differ in three important respects: first, they can have many more domains than the ANFs I and therefore can be extended over greater distance; second, the interpeak forces are lower, indicating a subtle difference in domain unfolding; and third, they are usually extended for a greater distance before they begin to resist extension (the average distance to the first peak is 656 nm vs. 188 nm for ANFs I) (Figs. 2 and 3, Table 1). ANFs III therefore provide the cell with an adhesive that has greater flexibility and can be extended over much greater distances than the ANFs I and II.

It must be remembered that all of these curves have been recorded from naturally occurring adhesive mucilage in its native state. Therefore we would expect some variability in the curves recorded because the tip can come into contact with a nanofiber at any point along its length. Furthermore the fibers themselves are unlikely to be arranged in a regular pattern that presents all of their ends toward the cantilever tip. When considering the complex nature of the overall adhesive mucilage, it is remarkable that we have recorded saw-tooth curves with such reproducible characteristics.

Purified single molecules of titin have been shown to preferentially form oligomers of six molecules representing a stable supramolecular arrangement when dispersed on a glass surface (9). AFM images of these molecules show that they form oligomers via head-to-head associations and when stretched mechanically behave as independent WLCs. A similar self-assembly may occur during the formation of the adhesive components of *T. undulatum*, either before secretion or immediately thereafter, within the forming mucilage pad. A key difference between the ANFs presented in this study and the supramolecular arrangement of titin molecules is that the interpeak distance of the saw-tooth curves stays constant and precise in this study when mechanically unfolded, whereas it does not for titin (9). The titin molecules were shown to associate only at their heads and otherwise appear independent. By contrast, the precise saw-tooth pattern shown in *T. undulatum* fibers suggests that the monomers are precisely aligned and are coordinated by precise intermolecular cross-linking along the length of the polymers. This more complex structure suggests that assembly may take place within the Golgi vesicles where assembly is likely to be controlled by the cell.

The range of curves presented here, and therefore the adhesive components that they represent, were not recorded in Dugdale et al. (1). This difference may be due to the sharper tips that were used in this study. This greater range of adhesive components provides evidence that the ANFs of *T. undulatum* may be composed of a single species of modular protein. Moreover, this is the first time that we are aware of that single modular proteins have been mechanically unfolded with AFM from a native, living system. This AFM

force spectroscopy study provides direct insights into the complex function and assembly of the adhesive biocomposite that *T. undulatum* uses to attach to the substratum without any knowledge of the chemical composition of the adhesive mucilage.

The authors thank John Lewis from Defense Science and Technology Organization (DSTO), Australian Department of Defense, and Paul Mulvaney from School of Chemistry, University of Melbourne, for valuable discussions and technical support.

The Australian Research Council and our industry partner Akzo Nobel, Gateshead, UK, provided funding (Industry Linkage Grant No. LP0454982). We also thank the Defense Science and Technology Organization (DSTO) of the Australian Department of Defense for financial assistance.

REFERENCES

1. Dugdale, T. M., R. Dagastine, A. Chiovitti, P. Mulvaney, and R. Wetherbee. 2005. Single adhesive nanofibers from a live diatom have the signature fingerprint of modular proteins. *Biophys. J.* 89: 4252–4260.
2. Picket-Heaps, J., A. Schmid, and L. A. Edgar. 1990. The cell biology of diatom valve formation. *In* Progress in Phycological Research. F. E. Round and D. J. Chapman, editors. Biopress Ltd., Bristol, UK. 1–168.
3. Hoagland, K. D., J. R. Rosowski, M. R. Gretz, and S. C. Roemer. 1993. Diatom extracellular polymeric substances: function, fine structure, chemistry and physiology. *J. Phycol.* 29:537–566.
4. Kooistra, W. H. C. F., M. De Stefano, D. G. Mann, N. Salma, and L. K. Medlin. 2003. Phylogenetic position of *Toxarium*, a pennate-like lineage within centric diatoms (Bacillariophyceae). *J. Phycol.* 39:185–197.
5. Bemis, J. E., B. B. Akhremitchev, and G. C. Walker. 1999. Single polymer chain elongation by atomic force microscopy. *Langmuir.* 15: 2799–2805.
6. Andersen, R. A., J. A. Berges, P. J. Harrison, and M. M. Watanabe. 2005. Recipes for freshwater and seawater media. *In* Algal Culturing Techniques. R. A. Andersen, editor. Elsevier Academic Press, Burlington, MA. 429–538.
7. Hutter, J. L., and J. Bechhoefer. 1993. Calibration of atomic force microscope tips. *Rev. Sci. Instrum.* 64:1868–1873.
8. Rief, M., F. Oesterhelt, B. Heymann, and H. Gaub. 1997. Single molecule force spectroscopy on polysaccharides by atomic force microscopy. *Science.* 275:1295–1297.
9. Kellermayer, M. S. Z., C. Bustamante, and H. L. Granzier. 2003. Mechanics and structure of titin oligomers explored with atomic force microscopy. *Biochim. Biophys. Acta.* 1604:105–114.
10. Kellermayer, M. S. Z., S. B. Smith, H. L. Granzier, and C. Bustamante. 1997. Folding-unfolding transitions in single molecules characterized with laser tweezers. *Science.* 276:1112–1115.
11. Crawford, S. A., M. J. Higgins, P. Mulvaney, and R. Wetherbee. 2001. Nanostructure of the diatom frustule as revealed by atomic force and scanning electron microscopy. *J. Phycol.* 37:543–554.
12. Gebeshuber, I. C., J. H. Kindt, J. B. Thompson, Y. Del Amo, H. Stachelberger, M. A. Brezezinski, G. D. Stucky, D. E. Morse, and P. K. Hansma. 2003. Atomic force microscopy of living diatoms in ambient conditions. *J. Microsc.* 212:292–299.
13. Gebeshuber, I. C., J. B. Thompson, Y. Del Amo, H. Stachelberger, and J. H. Kindt. 2002. In vivo nanoscale atomic force microscopy investigation of diatom adhesive properties. *Mater. Sci. Technol.* 18: 763–766.
14. Higgins, M. J., S. A. Crawford, P. Mulvaney, and R. Wetherbee. 2002. Characterisation of the adhesive mucilages secreted by live diatom cells using atomic force microscopy. *Protist.* 153:25–38.
15. Higgins, M. J., P. Molino, P. Mulvaney, and R. Wetherbee. 2003. The structure and nanomechanical properties of the adhesive mucilage that mediates diatom:substratum adhesion and motility. *J. Phycol.* 39: 1181–1193.
16. Higgins, M. J., J. E. Sader, P. Mulvaney, and R. Wetherbee. 2003. Probing the surface of living diatoms with atomic force microscopy: the nanostructure and nanomechanical properties of the mucilage layer. *J. Phycol.* 39:722–734.
17. Callow, J. A., S. A. Crawford, M. J. Higgins, P. Mulvaney, and R. Wetherbee. 2000. The application of atomic force microscopy to topographical studies and force measurements on the secreted adhesive of the green alga Enteromorpha. *Planta.* 211:641–647.
18. Camesano, T. A., and N. I. Abu-Lail. 2002. Heterogeneity in bacterial polysaccharides, probed on a single molecule basis. *Biomacromolecules.* 3:661–667.
19. Benoit, M., D. Gabriel, G. Gerisch, and H. E. Gaub. 2000. Discrete interactions in cell adhesion measured by single-molecule force spectroscopy. *Nat. Cell Biol.* 2:313–317.
20. Touhami, A., B. Hoffmann, A. Vaslla, F. A. Denis, and Y. F. Dufrene. 2003. Aggregation of yeast cells: direct measurements of discrete lectin-carbohydrate interactions. *Microbiology.* 149:2873–2878.
21. van der Aa, B. C., M. Asther, and Y. F. Dufrene. 2001. Surface properties of Aspergillus oryzae spores investigated by atomic force microscopy. *Colloids Surf. B Biointerfaces.* 24:277–278.
22. Li, H., and J. M. Fernandez. 2003. Mechanical design of the first proximal Ig domain of human cardiac titin revealed by single molecule force spectroscopy. *J. Mol. Biol.* 334:75–86.
23. Li, H., A. F. Oberhaser, S. D. Redick, M. Carrion-Vazquez, and H. P. Erickson. 2001. Multiple conformations of PEVK proteins detected by single-molecule techniques. *Proc. Natl. Acad. Sci. USA.* 98: 10682–10686.
24. Sarkar, A., S. Caamano, and J. M. Fernandez. 2005. The elasticity of individual titin PEVK exons measured by single molecule atomic force microscopy. *J. Biol. Chem.* 280:6261–6264.
25. Schoenauer, R., P. Bertoncini, G. Machaidze, U. Aebi, J.-C. Perriard, M. Hegner, and I. Agarkova. 2005. Myomesin is a molecular spring with adaptable elasticity. *J. Mol. Biol.* 349:367–379.
26. Rief, M., M. Gautel, A. Schemmel, and H. E. Gaub. 1998. The mechanical stability of immunoglobulin and fibronectin III domains in the muscle protein titin measured by atomic force microscopy. *Biophys. J.* 75:3008–3014.
27. Oberhauser, A. F., C. Badilla-Fernandez, M. Carrion-Vazquez, and J. M. Fernandez. 2002. The mechanical hierarchies of fibronectin observed with single-molecule AFM. *J. Mol. Biol.* 319:433–447.
28. Marszalek, P. E., H. Li, and J. M. Fernandez. 2001. Fingerprinting polysaccharides with single-molecule atomic force microscopy. *Nat. Biotechnol.* 19:258–262.